MHD simulations of impurity transport during sawteeth for ASDEX-Upgrade plasmas

J.-H. Ahn[1], X. Garbet[1], R. Guirlet[1], O. Février[1], H. Lütjens[2], M. Sertoli[3],
the ASDEX-Upgrade Team and the EUROfusion MST1 Team*

[1] *CEA, IRFM, F-13108 Saint Paul-lez-Durance, France*

[2] *Centre de Physique Théorique, Ecole Polytechnique, CNRS, F-91128 Palaiseau, France*

[3] *Max Planck Institut für Plasmaphysik, Boltzmannstraße 2, D-85748 Garching, Germany*

Introduction

Several tokamaks are now equipped with Tungsten plasma facing components (PFCs) to prepare the operation of ITER. It has been observed that in some conditions, the accumulation of Tungsten in core plasmas may lead to a radiative collapse due to excessive cooling. Hence, the control of heavy impurity transport has become a subject of renewed interest. RF heating appears to be a useful tool for preventing accumulation. However, in core plasmas, the precise mechanism has not been fully understood yet as it involves neoclassical and turbulent transport combined with sawtooth dynamics. In a number of experiments, it has already been shown that a sawtooth collapse induces a sudden radial transport of impurities, more specifically an impurity flux between edge and core plasma [1].

This paper presents intermediate steps towards the modelling of impurity behaviour during sawtooth cycles observed in an ASDEX-Upgrade discharge with a central ECRH deposition [2], performed during the EUROfusion MST1 2014 campaign. Fluid equations for impurities in the high collisional regime have been derived to describe the effects of neoclassical transport. This model has been implemented in the XTOR-2F code [3] in order to be coupled with nonlinear MHD equations for plasma electrons and ions. Also, preliminary results on the effects of a RF-like heat source on impurity transport are presented.

Impurity transport model coupled with MHD equations

Heavy impurities are in the Pfirsch-Schlüter collisional regime due to their high charge numbers, while the main ion species remains in the banana-plateau collisional regime in core plasmas. In this framework, the neoclassical theory predicts that the ion temperature gradient drives an outward convection, and is thus responsible for a favorable screening effect [4].

The fluid equations (Eq. (1) and (2)) for impurities corresponding to this case have then been implemented in the XTOR-2F code

$$\partial_t n_z + \nabla.(n_z \mathbf{V}_z) + \frac{\nabla p_z}{Ze}.\nabla \times \frac{\mathbf{B}}{B^2} = \nabla.\left(D_z^{turb}\nabla n_z - \mathbf{V}_{p,z}^{turb} n_z\right) + S_z \tag{1}$$

$$\partial_t V_{\parallel,z} = -\frac{\nabla_\parallel p_z}{m_z n_z} - \frac{Ze\nabla_\parallel \phi}{m_z} - \nu_{zi}\left(V_{\parallel,z} - V_{\parallel,i}\right) + \frac{3}{5}\frac{Z^2}{m_z}\nabla_\parallel T_i \tag{2}$$

in addition to the fluid equations that describe the plasma electrons and ions [3]. The diffusion

*See http://www.euro-fusionscipub.org/mst1

coefficient D_z^{turb} and the pinch velocity $\mathbf{V}_{p,z}^{turb}$ on the R.H.S. of Equation (1) correspond to the contribution of turbulent transport, and are defined as radial functions constant in time. It can be shown that this model reproduces well the neoclassical impurity transport, including the thermal screening. In fact, the term corresponding to the thermal screening can be derived from the expression of the thermal force between the main ion species and impurity. This model allows one to study the combined effect of collisional transport and sawtooth-induced transport of impurities in the Pfirsch-Schlüter regime.

Since the neoclassical time scales are larger than the time scales of MHD instabilities, neoclassical quantities are averaged on magnetic flux surfaces, denoted with angled brackets. With the previous fluid equations (Eq. (1) and (2)), the radial projection of neoclassical impurity flux is derived and can be written as

$$\langle \Gamma_z . \nabla r \rangle = -D_z^{neo} n_z \left(\partial_r \ln n_z - Z \partial_r \ln n_i - ZH \partial_r \ln T_i \right) \tag{3}$$

where the constant $H \simeq -0.5$ for impurities in the Pfirsch-Schlüter regime and the main ion species in the banana-plateau regime [5].

XTOR-2F simulation results

In a first stage, simulations without kink, in a circular cross section, have been performed in order to verify the neoclassical transport model which has been implemented in fluid equations. To facilitate the monitoring of impurity transport, a flat profile was chosen for the initial impurity density. Also, analytical initial profiles of ion density and temperature are chosen and represented in Figure 1. It is expected that only the screening effect due to the temperature gradient appears in the region $r/a < 0.4$, where the ion density profile is flat. Figure 2-a shows that the model without the thermal force induces an inward flux of impurity due to the ion density gradient. However, the thermal force in the fluid equations clearly produces an outward impurity flux (Fig. 2-b). This test confirms that the fluid equations analytically derived and implemented in the XTOR-2F code reproduces the well known temperature screening effect as predicted by the neoclassical theory.

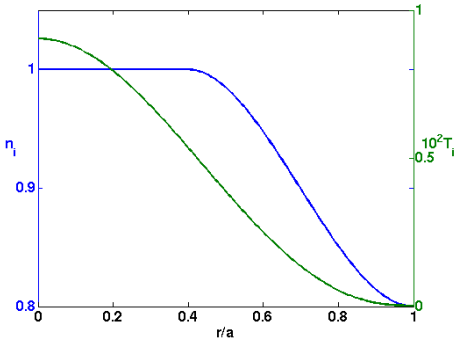

Figure 1: The initial ion density profile (blue) and temperature profile (green) in XTOR-2F units

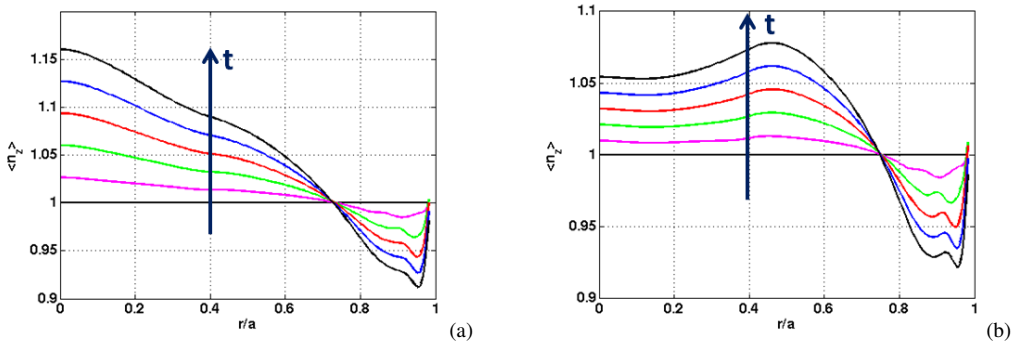

Figure 2: Time evolution of the surface averaged impurity density (a) without and (b) with thermal force in the model (Each colour corresponds to a time point).

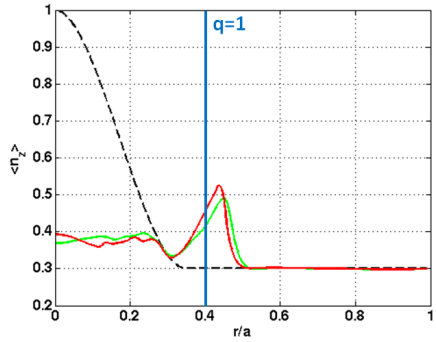

Figure 3: Surface averaged impurity density before (dashed lines) and after (solid lines) sawtooth crash for model without (green) and with (red) temperature screening.

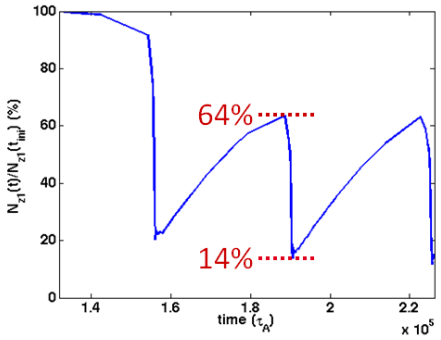

Figure 4: Time Evolution of the relative impurity quantity inside the volume V_1 delimited by the $q = 1$ surface (*cf.* Eq. (4)).

Figure 3 shows the impurity density evolution during a sawtooth crash from XTOR-2F simulations with the implemented model. An arbitrary peaked impurity profile is chosen at the beginning to highlight the temperature screening effect. The comparison of two cases, without and with temperature screening, reflects no remarkable difference in the impurity behaviour during the sawtooth crash, since the MHD time scale is much smaller than the neoclassical transport time scale. Figure 4 shows the time evolution of the ratio $N_{z1}(t)/N_{z1}(t_{ini})$, where the quantity $N_{z1}(t)$ is defined as

$$N_{z1}(t) = \int_{V_1} \left(n_z(\mathbf{r},t) - n_z(r_{q=1},t_{ini}\right) d^3\mathbf{r} \tag{4}$$

to assess the impurity content inside the plasma volume V_1 delimited by the $q = 1$ surface [6]. This quantity allows to trace and quantify the effects of the neoclassical transport which will appear after several sawtooth cycles in ongoing simulations.

In the XTOR-2F code, a heat source is added in the energy equation to model RF heating in the plasma. The propagation model of the heat source is identical to the one implemented for current drive [7]. However, this additional heat source does not precisely reflect ECRH nor ICRH deposition in experiments, as the actual XTOR-2F energy equation is written for total pressure. Thus, the heat source is considered to be equally distributed to plasma electrons and ions. A simulation without kink with a Gaussian heat source on the magnetic axis was performed, in order to test its effects on the impurity transport. Again, a flat profile was chosen for the initial impurity density to monitor the impurity transport. Figure 5 shows that, when an on-axis heat source is applied, impurities are depleted from the near-axis region of the plasma compared to the case without heat source (Fig. 2-b). Further analysis is necessary in order to understand how the applied heat source affects the MHD quantities and the impurity transport properties.

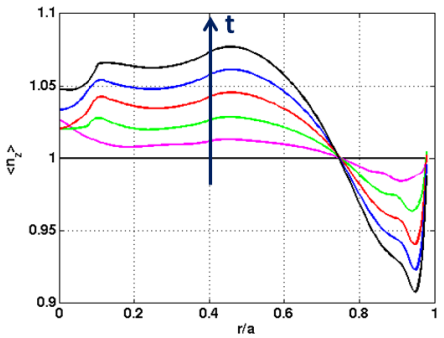

Figure 5: Time evolution of surface averaged impurity density when a heat source is applied on the magnetic axis (Each colour corresponds to a time point).

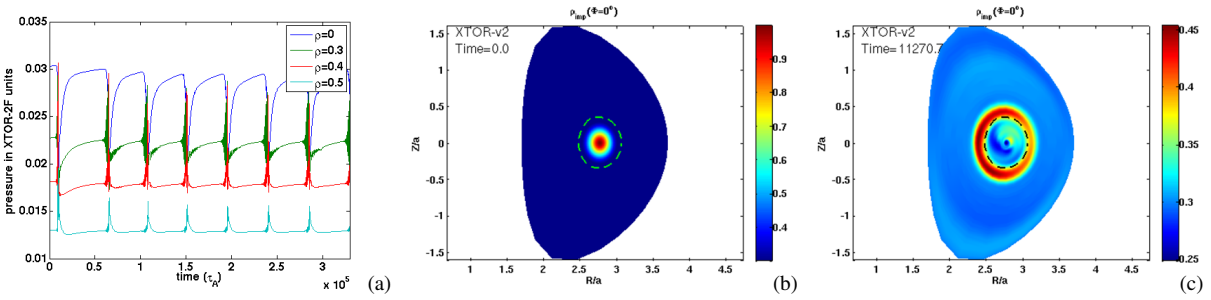

Figure 6: XTOR-2F simulation of sawteeth in an elongated geometry ($\kappa = 1.6$, $\delta = 0.4$). (a) Time evolution of pressure in different radial positions. Impurity density contours (b) before and (c) after sawtooth crash.

The XTOR-2F code has been shown to simulate sawtooth cycles in fair agreement with some experiments in circular cross section [8]. However, simulations of sawtooth cycles in a non-circular cross section have not been done yet. It is well known that the plasma elongation strongly destabilizes the kink mode [9]. A full scan of XTOR-2F input parameters has then been done to simulate stationary sawtooth cycles in an elongated cross section (Fig. 6-a). It is shown that the implemented model (Eq. (1) and (2)) gives the same impurity behaviour in an elongated cross section (Fig. 6-b and 6-c) as simulations in a circular cross section. Simulations in an elongated cross section will allow to compare the model with ASDEX-Upgrade discharges.

Conclusion and prospect

The XTOR-2F code has been modified to model impurity transport in the Pfirsch-Schlüter regime. Simulations show that the model reproduces the temperature screening effect as predicted by the neoclassical theory. Impurity transport is dominated by MHD convection during the sawtooth crash phase, as an effect of collisional transport is expected on a longer time scale. Thus, simulations of a large number of successive sawtooth cycles are ongoing to assess the interplay between the neoclassical transport and sawteeth. A full scan of input parameters allowed the XTOR-2F code to simulate sawteeth in an elongated cross section. It is also observed in simulations that the presence of a heat source tends to deplete core impurities.

With all these ingredients, plasma scenarios similar to the referred ASDEX-Upgrade discharge [2] will be simulated. Theses studies will allow to provide more physical understanding of the impurity dynamics and control for an efficient operation in future fusion devices.

➤*Numerical resources were provided by CINES, IDRIS and TGCC of GENCI (x2015056348), Mésocentre of Aix-Marseille University (15b025), Helios of IFERC-CSC (MaCoToP).*
➤*This work has been carried out within the framework of the EUROfusion Consortium and has received funding from the Euratom research and training programme 2014-2018 under grant agreement No 633053. The views and opinions expressed herein do not necessarily reflect those of the European Commission.*

References

[1] R. Dux et al., *Nucl. Fus.* **39** 1509 (1999)
[2] M. Sertoli et al., *this conference*, O4.129
[3] H. Lütjens and J.-F. Luciani, *J. Comp. Phys.* **229** 8130 (2010)
[4] P. Helander and D.J. Sigmar, *Cambridge Univ. Press* (2002)
[5] S.P. Hirshman and D.J. Sigmar, *Nucl. Fus.* **21** 1079 (1981)
[6] T. Nicolas et al., *Phys. Plasmas* **21** 012507 (2014)
[7] O. Février et al., *this conference*, P1.104
[8] T. Nicolas et al., *Phys. Plasmas* **19** 112305 (2012)
[9] H. Lütjens et al., *Nucl. Fus.* **32** 1625 (1992)